Low-Valent Titanium Species Stabilized with Aluminum/Boron Hydride Fragments

Estefanía del Horno,[a] Jesús Jover,*[b] Miguel Mena,[a] Adrián Pérez-Redondo,[a] and Carlos Yélamos*[a]

[a] E. del Horno, Dr. M. Mena, Dr. A. Pérez-Redondo, Prof. Dr. C. Yélamos, Departamento de Química Orgánica y Química Inorgánica, Instituto de Investigación Química "Andrés M. del Río" (IQAR), Universidad de Alcalá, 28805 Alcalá de Henares-Madrid (Spain). E-mail: carlos.yelamos@uah.es

[b] Dr. J. Jover, Secció de Química Inorgànica, Departament de Química Inorgànica i Orgànica, Institut de Química Teòrica i Computacional (IQTC-UB), Universitat de Barcelona, Martí i Franquès 1-11, 08028 Barcelona (Spain). E-mail: jjovermo@ub.edu

Dedication: Dedicated to the memory of Prof. Dr. Carolina Burgos, who passed away in September 2020.

Keywords: aluminum • boron • density functional calculations • reduction • titanium

Abstract:

Low-valent titanium species were prepared by reaction of [TiCp*X_3] (Cp* = η^5-C_5Me_5; X = Cl, Br, Me) with $LiEH_4$ (E = Al, B) or BH_3(thf), and their structures elucidated by experimental and theoretical methods. The treatment of trihalides [TiCp*X_3] with $LiAlH_4$ in ethereal solvents (L) leads to the hydride-bridged heterometallic complexes [{TiCp*(μ-H)}$_2${(μ-H)$_2$AlX(L)}$_2$] (L = thf, X = Cl, Br; L = OEt_2, X = Cl). Density functional theory (DFT) calculations for those compounds reveal an open-shell singlet ground state with a Ti–Ti bond and can be described as titanium(II) species. The theoretical analyses also show strong interactions between the Ti–Ti bond and the empty *s* orbitals of the Al atom of the AlH_2XL fragments, which behave as σ-accepting (Z-type) ligands. Analogous reactions of [TiCp*X_3] with $LiBH_4$ (2 and 3 equiv) in tetrahydrofuran at room temperature and at 85 ºC lead to the titanium(III) compounds [{TiCp*(BH_4)(μ-X)}$_2$] (X = Cl, Br) and [{TiCp*(BH_4)(μ-BH_4)}$_2$], respectively. The treatment of [TiCp*Me_3] with 4 and 5 equiv of BH_3(thf) produces the diamagnetic [{TiCp*(BH_3Me)}$_2$(μ-B_2H_6)] and paramagnetic [{TiCp*(μ-B_2H_6)}$_2$] complexes, respectively.

Introduction

The chemistry of titanium is characterized by the preponderance of combinations containing the highest oxidation state for this metal (IV, d^0 configuration), by far the most stable in comparison with the highly reactive low valences, such as III (d^1) and II (d^2). Nonetheless, low-valent titanium complexes are of great interest due to their implication in bond-forming reactions and small-molecule activation useful in synthesis and catalysis.[1,2,3] For instance, titanium(III) reagents are frequently used in catalytic single-electron transfers for organic synthesis.[2,4] In addition, catalytic C–X (X = C, O, B, N) coupling reactions involving redox events at titanium(II) centers are well-documented in the literature.[1,5]

A typical protocol for accessing low-valent titanium species is the reaction of titanium(IV) halide or alkoxide precursors with a reducing metal (e.g., alkali metals, Zn, Mg, Mn, Al) or their derivatives (e.g., LiR, MgClR, KC_8).[2,6] Alternatively, Mashima and co-workers have developed salt-free methodologies by using milder organosilane reductants for the preparation of titanium(III) chloride compounds with applications for C–C bond formation.[3] For example, this reduction method allowed the clean synthesis of the bis(cyclopentadienyl)titanium(III) chloride [$Ti(\eta^5\text{-}C_5H_5)_2Cl$] (Nugent-RajanBabu reagent)[4] and the half-sandwich titanium(III) dichloride [$TiCp^*Cl_2$] ($Cp^* = \eta^5\text{-}C_5Me_5$) compounds without reductant-derived metal salts which are typical contaminants in conventional reduction protocols.[7] While [$Ti(\eta^5\text{-}C_5H_5)_2Cl$] and its derivatives with small R substituents on the cyclopentadienyl rings have been stablished as chloride-bridged dimers [$\{Ti(\eta^5\text{-}C_5H_{5-n}R_n)_2(\mu\text{-}Cl)\}_2$] in the solid state,[8] the structures and properties of monocyclopentadienyltitanium(III) dihalides [$Ti(\eta^5\text{-}C_5R_5)Cl_2$] have remained poorly described in the literature for decades.[9] Noteworthy, [$Ti(\eta^5\text{-}C_5R_5)X_2$] derivatives are receiving considerable interest as catalysts in organic synthesis in recent years.[10] The

lack of structural information led us to reexamine monocyclopentadienyltitanium(III) dihalide complexes and we recently reported the crystal and electronic structures of titanium(III) aggregates of composition [{TiCp*Cl_2}$_n$] (n = 2, 3) prepared by thermolysis or hydrogenolysis of the monomethyltitanium(IV) compound [TiCp*Cl_2Me].[11]

In a more general procedure, half-sandwich titanium(III) dihalide complexes with halide-bridged dimeric structures [{TiCp*X(μ-X)}$_2$] (X = Cl, Br, I) could be obtained, although in lower yields, by reduction of trihalide complexes [TiCp*X_3] with $LiAlH_4$ in toluene.[12] The strong reductant lithium tetrahydridoaluminate has been previously used to generate low-valent titanium catalysts and reagents for various organic transformations.[13] The structure of the active species is not usually identified but several heterobimetallic bridged hydrides with the Ti(III)–H–Al motif have been isolated by salt metathesis from titanium(IV) precursors and aluminum hydrides.[14,15,16] In particular, within a broad study on the reaction of cyclopentadienyltitanium complexes with $LiAlH_4$,[15] Bulychev and co-workers investigated by calorimetric titration and EPR techniques the interactions of [Ti(η^5-C_5H_5)Cl_3] with variable ratios of $LiAlH_4$ but titanium-aluminum products were not isolated.[17] In comparison, a well-stablished route for stable tetrahydridoboratotitanium(III) derivatives containing Ti(III)–H–B bridges is the treatment of titanium(IV) halides with the milder reductant lithium tetrahydridoborate $LiBH_4$.[18] Interestingly, the reactions of monocyclopentadienyl metal chlorides of transition metals of groups 5-9 with monoborane precursors ($LiBH_4$ or BH_3(thf)) are efficient routes to metallaboranes.[19]

Studies on the reaction of group 13 hydride complexes, especially sodium alanate $NaAlH_4$, with titanium compounds are also relevant in the context of hydrogen storage. Since Bogdanovic and Schwickardi reported that Ti-doped sodium alanate could enhance reversible hydrogen storage under moderate conditions,[20] many titanium compounds

(i.e., $TiCl_3$, TiF_3, $Ti(OBu)_4$, TiH_2) have been tested as catalyst in those processes.[21] The results revealed that the titanium atoms in the precursors are reduced by $NaAlH_4$ to a low-valent or even zerovalent state.[21,22]

As part of a project devoted to the study the structure and properties of low-valent monocyclopentadienyltitanium hydride complexes, we recently communicated the synthesis and electronic structure of bi- and trimetallic titanium(III) compounds containing unprecedented BN ligands, namely $(NH_2BH_2NHBH_3)^{2-}$ and $\{N(BH_3)_3\}^{3-}$, from the reaction of $[TiCp^*Me_3]$ with NH_3BH_3.[23] Here we report the syntheses, crystal structures, and electronic structures of several titanium(II) and titanium(III) species prepared by reaction of $[TiCp^*X_3]$ (X = Cl, Br, Me) with $LiEH_4$ (E = Al, B) or BH_3(thf).

Results and Discussion

Treatment of the titanium(IV) complexes $[TiCp^*X_3]$ (X = Cl, Br)[24] with two equivalents of lithium tetrahydridoaluminate in tetrahydrofuran at room temperature produced an immediate color change from red to dark-blue with vigorous gas evolution. Upon workup of the reaction mixtures, the hydride-bridged titanium(II)-aluminum heterometallic derivatives $[\{TiCp^*(\mu\text{-}H)\}_2\{(\mu\text{-}H)_2AlX(thf)\}_2]$ (X = Cl (**1**), Br (**2**)) were obtained (Scheme 1). Compounds **1** and **2** were isolated in 85 and 62% yields as extremely air-sensitive dark-blue solids, which exhibit a good solubility in hydrocarbon solvents. Analogous treatment of $[TiCp^*Cl_3]$ with $LiAlH_4$ (2 equiv) in diethyl ether gave $[\{TiCp^*(\mu\text{-}H)\}_2\{(\mu\text{-}H)_2AlCl(OEt_2)\}_2]$ (**3**). In contrast to blue compounds **1** and **2**, complex **3** was isolated from the reaction as a brown powder, and satisfactory elemental analyses could not be obtained. Crystallization in hexane at –35 ºC gave a very small fraction of dark-blue crystals of $\mathbf{3}\cdot 0.5C_6H_{14}$, which were used for NMR spectroscopy characterization and an X-ray crystal structure determination.

Noteworthy, the treatment of [TiCp*Cl_3] with one equivalent of $LiAlH_4$ in tetrahydrofuran gave a mixture of complex **1** and the starting material [TiCp*Cl_3], while we have previously reported that the reaction in toluene afforded the green dimeric titanium(III) complex [{TiCp*Cl(μ-Cl)}$_2$].[12] The latter dichloride complex dissolves in tetrahydrofuran to give a green-blue solution of the adduct [TiCp*Cl_2(thf)],[11] which readily reacts with $LiAlH_4$ to form a dark-blue solution of complex **1** with gas evolution. Most likely, the reaction proceeds by metathesis of one chloride ligand of [TiCp*Cl_2(thf)] by a tetrahydridoaluminato group and subsequent reduction of the Ti(III) center to Ti(II), presumably by molecular hydrogen formation, and the remaining Cl atom was transferred to the aluminum center.

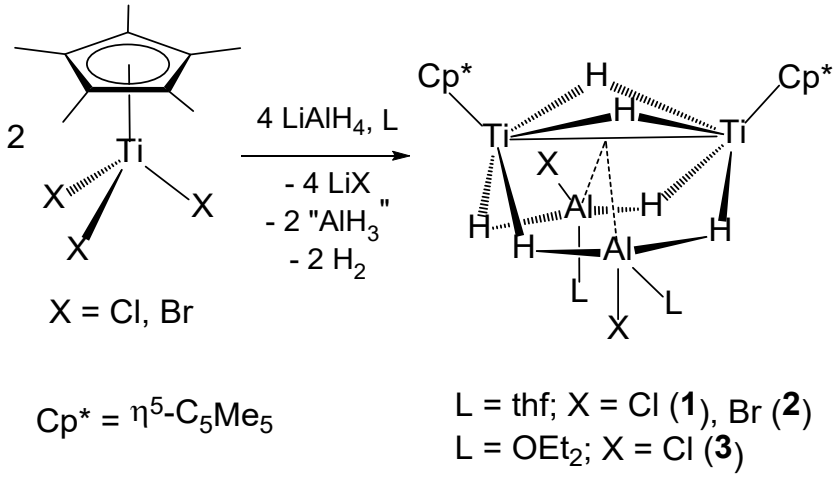

Scheme 1. Reactions of [TiCp*X_3] with $LiAlH_4$ in ethereal solvents (L).

The molecular structure of **1** is shown in Figure 1, whereas those of the analogous complexes **2** and **3** are presented in Figures S1 and S2 of the Supporting Information.[25] Selected distances and angles of complexes **1**–**3** are compared in Table 1. The crystal structures of complexes **1**–**3** show dimers with two [Ti(η^5-C_5Me_5)] moieties held together by two bridging hydride ligands. The [Ti(μ-H)$_2$Ti] fragments exhibit a butterfly structure with averaged Ti–H bond lengths of 1.85(2) Å and Ti–H–Ti angles of 99(1)º. In addition,

the titanium atoms are linked by two {(μ-H)$_2$AlXL} bridging groups. Thus, each titanium atom exhibits a four-legged piano-stool geometry with angles H–Ti–H in the range 73(1)-132(2)º. The titanium–titanium distances in complexes **1**–**3** of averaged 2.823(3) Å are shorter than that found in titanium metal (2.896 Å).[26]

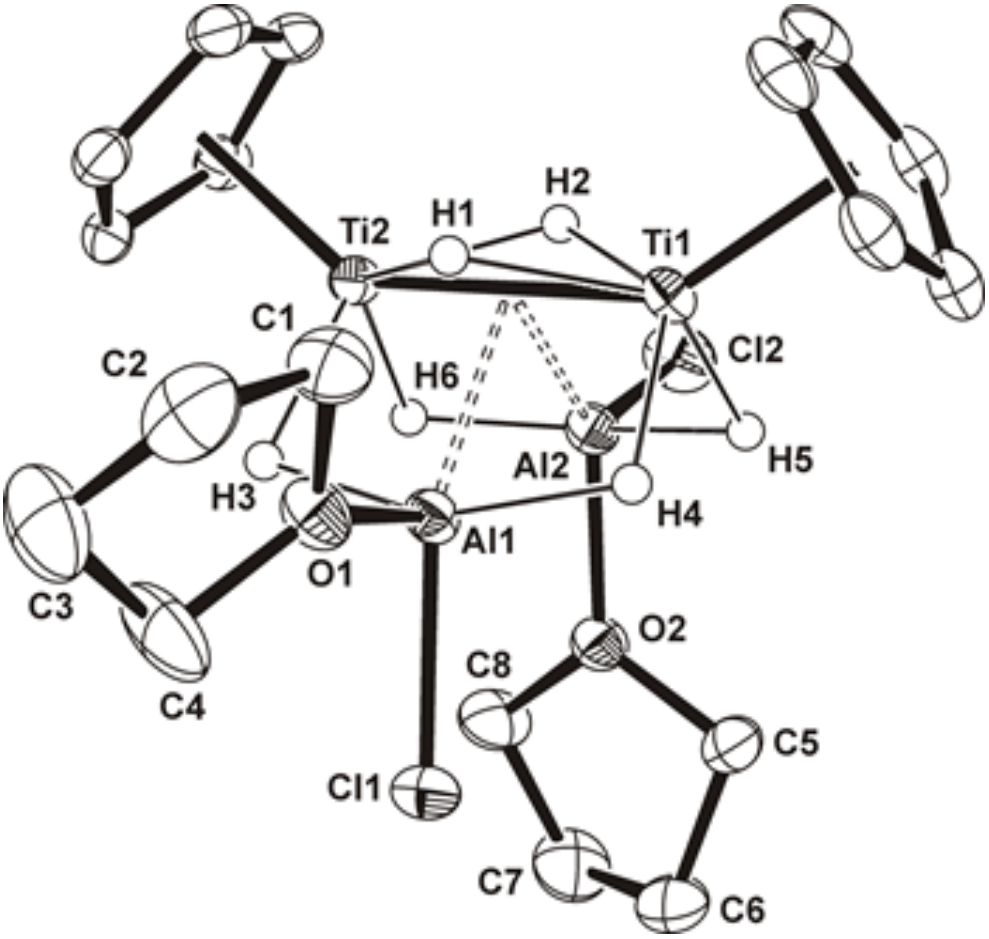

Figure 1. Perspective view of **1** with thermal ellipsoids at the 50% probability level. Methyl groups of the η^5-C$_5$Me$_5$ and hydrogen atoms of tetrahydrofuran ligands are omitted for clarity.

Table 1. Selected Averaged Lengths (Å) and Angles (deg) for Complexes **1**-**3**

	1 (X = Cl; L = thf)	**2** (X = Br; L = thf)	**3** (X = Cl; L= OEt_2)
Ti–Ti	2.822(1)	2.827(1)	2.821(1)
Ti–Al	2.644(12)	2.641(12)	2.648(10)
Ti–H(Ti)	1.83(2)	1.85(1)	1.86(1)
Ti–H(Al)	1.82(1)	1.85(2)	1.81(4)
Al–H(Ti)	1.64(4)	1.66(3)	1.66(2)
Al–X	2.169(1), 2.196(1)	2.344(2), 2.369(2)	2.184(4)
Al–O	1.887(2), 1.915(2)	1.886(3), 1.910(3)	1.910(9)
H(1)–Ti–H(2)	74(1)	75(1)	76(1)
Ti–H–Ti	100(1)	100(1)	98(1)

Each aluminum atom in **1**–**3** shows a four coordinate environment and adopts a polyhedral geometry of distorted trigonal pyramidal (τ_4 = 0.75–0.77, perfect trigonal pyramidal geometry gives τ_4 = 0.85).[27] The L ligands are located at the apical position of the pyramid, but occupy different geometrical sites in the crystal structures. In addition, complexes **1**-**3** display titanium–aluminum distances of averaged 2.644(10) Å, which are less than the sum of covalent radii (2.81(9) Å)[28] and significantly shorter than those reported for heterometallic compounds incorporating Ti(III)–H–Al motifs.[15,16] These short Ti–Al separations could be indicative of metal–metal bonding (vide infra).

In accord with the nearly C_s symmetry found in the solid-state structure, the ^{1}H and $^{13}C\{^1H\}$ NMR spectra of complexes **1**-**3** in [D_6]benzene at room temperature reveal resonance signals for two equivalent η^5-C_5Me_5 ligands and those expected for two non-equivalent tetrahydrofuran or diethyl ether molecules. The resonances in the ^{1}H NMR spectra are slightly broad and those due to the hydride ligands could not be observed.

Density functional theory (DFT) studies were conducted to establish the electronic structure of compounds **1** and **2**. The computed geometries are in good agreement with the crystallographic data (see Tables S3 and S4 in the Supporting Information). The electronic structures of these dinuclear complexes are best described as open-shell singlets in which an additional Ti–Ti bond has been established (Figure 2a). The oxidation state for both titanium atoms seems to match the expected titanium(II) prediction.

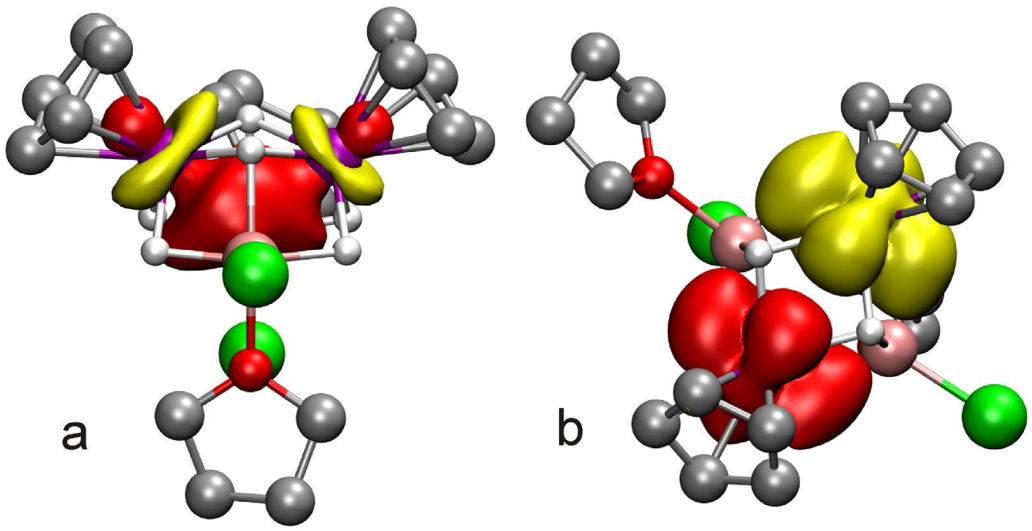

Figure 2. a) 3D representation of the MO for compound **1** showing the Ti–Ti bond; b) Representation of the spin density for compound **1**. Methyl groups of the η^5-C_5Me_5 ligands are omitted for clarity.

The electronic structure can be confirmed by the computed Natural Bond Orbital (NBO) analysis; in which it can be found the expected Ti–Ti bond and the SOMOs containing the unpaired electrons (Figure S5). The spin density shows opposed signs for each transition metal center (Figure 2b). These calculations and the subsequent NBO analysis ratify that the Ti atoms can be described as titanium(II). Interestingly, complexes **1** and **2** show also some donor/acceptor NBO interactions in addition to the usual Ti–H→Ti

interactions (Figure 3a). Thus, the calculations reveal two very strong interactions between the Ti–Ti bond and the empty *s* orbitals of the Al atoms (Figure 3b), which may contribute to the stabilization of the whole compound. These titanium→aluminum interactions are unprecedented in the literature, although there are many examples of low-valent electron-rich late transition metals (TM) with Lewis acids (LA) moieties (based on group 13, 14, 15 or 16 elements) which show TM→LA interactions.[29] The Lewis acids behave as σ-acceptor (Z-type) ligands toward many late transition metal in low oxidation state, but in complexes **1**–**3** the Lewis base donor is the pair of electrons involved in the Ti–Ti bond.

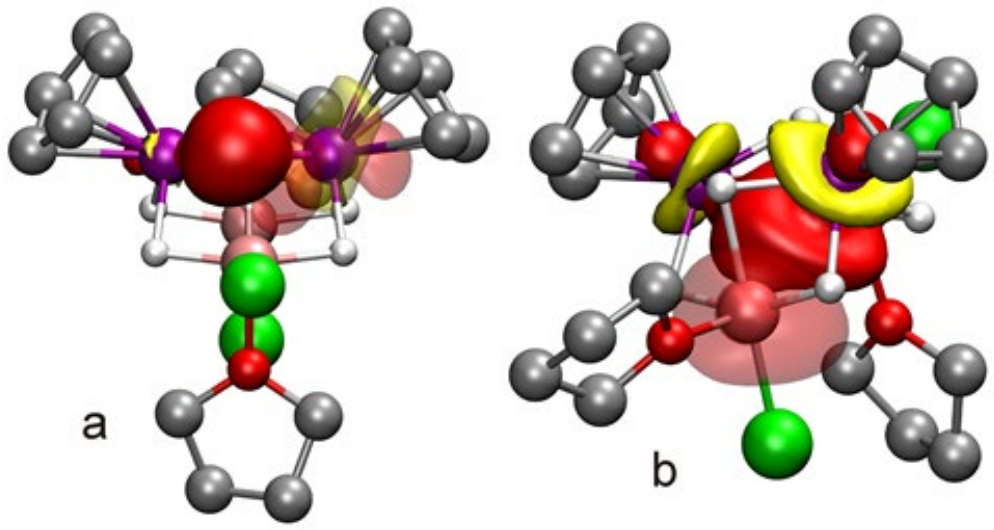

Figure 3. Donor/acceptor interactions between a) Ti–H→Ti and b) Ti–Ti→Al in compound **1**. Solid and transparent orbitals represent electron donor (full) and acceptor (empty) orbitals, respectively. Methyl groups of the η^5-C_5Me_5 ligands are omitted for clarity.

Noteworthy, our group has recently reported the isolation of the low-valent titanium trinuclear hydride complex [{TiCp*(μ-H)}$_3$(μ$_3$-H)(μ$_3$-NMe_2BH_2)] (Figure 4) in the

reaction of [TiCp*(CH_2SiMe_3)$_3$] with excess $NHMe_2BH_3$.[30] While this compound was initially described as a mixed valence Ti(II)/Ti(III) complex based on the total negative charges (7–) of the η^5-C_5Me_5 and μ_n-H ligands, subsequent DFT calculations indicated that the titanium atoms are in the oxidation state III.[23] The NBO analysis also showed bonding interactions between the titanium atoms and the B atom, which exhibits a certain extra electron density (0.7 e^-). After analysis of the Ti–Ti→Al bonding interaction determined in complexes **1** and **2**, we suggest that the more electronegative B atom could behave as such stronger σ-acceptor (Z-type) of electron density from a Ti–Ti (d^2-d^2) bond that results in formation of two titanium(III) units (2 d^1) units (Figure 4).[29b,31]

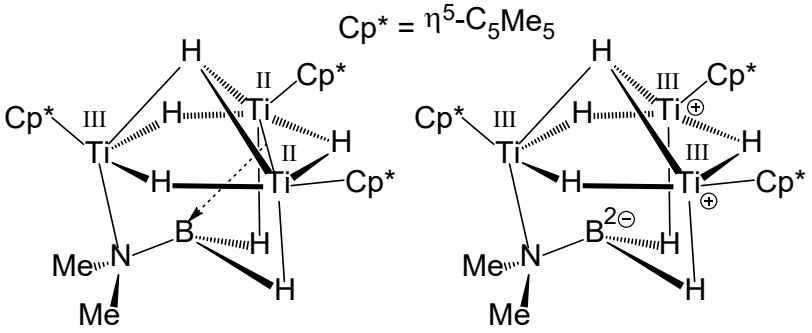

Figure 4. Two models contributing to the Ti–Ti→B bonding in complex [{TiCp*(μ-H)}$_3$(μ_3-H)(μ_3-NMe_2BH_2)].

We have also studied the reaction of titanium(IV) complexes [TiCp*X_3] (X = Cl, Br) with lithium tetrahydridoborate (Scheme 2). The treatment of [TiCp*X_3] with $LiBH_4$ (2 equiv) in tetrahydrofuran at room temperature led to blue solutions of presumably the titanium(III) complex [TiCp*(BH_4)X(thf)]. After vacuum elimination of tetrahydrofuran and subsequent extraction with toluene, the halide-bridged dimeric titanium(III)

tetrahydridoborato complexes [{TiCp*(BH_4)(μ-X)}$_2$] (X = Cl (**4**), Br (**5**)) were obtained. Compounds **4** and **5** were isolated in good yield (62 and 74%, respectively) as green solids, which are very soluble in hydrocarbon solvents. In contrast, the reaction of [TiCp*Cl_3] with excess $LiBH_4$ (≥ 3 equiv) in tetrahydrofuran at 85 ºC led to a blue solution of the mononuclear adduct [TiCp*(BH_4)$_2$(thf)] (**6**). The high solubility of **6** in tetrahydrofuran precluded the isolation of a solid sample of **6** from this solution, but it could be isolated, although in low yield (26%), as dark-blue crystals from a saturated toluene/tetrahydrofuran/hexane (2/2/1) solution at –35 ºC. The attempted sublimation of **6** (75 ºC, 0.1 Torr) afforded huge dark-blue crystals of the tetrahydrofuran-free dinuclear titanium(III) bis(tetrahydridoborato) complex [{TiCp*(BH_4)(μ-BH_4)}$_2$] (**7**) in 41% yield. Interestingly, complex **7** was easily prepared in higher yield (80%) by the direct reaction of [TiCp*Cl_3] with finely powdered $LiBH_4$ (≥ 3 equiv) in toluene at room temperature (Scheme 2).

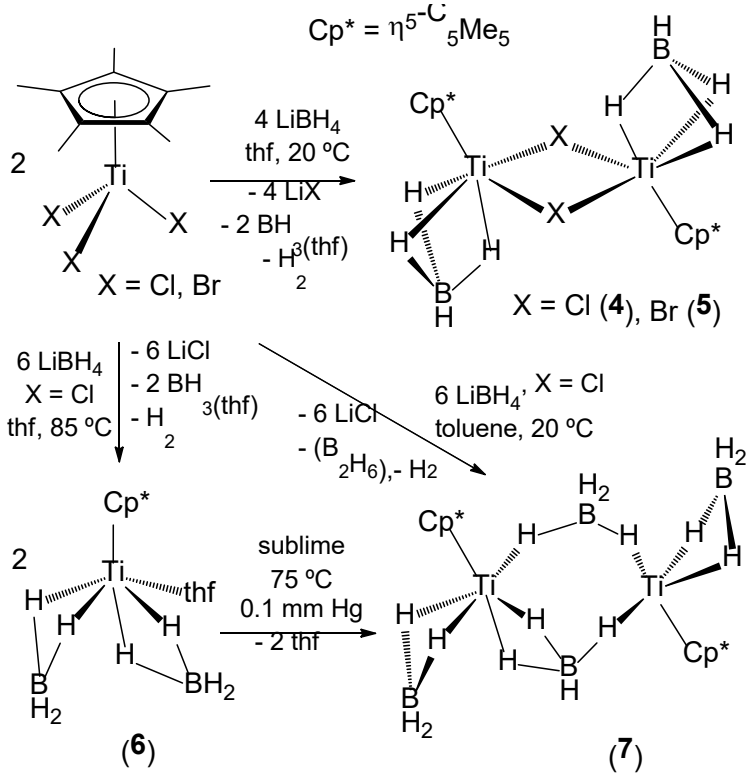

Scheme 2. Reactions of [TiCp*X_3] with $LiBH_4$.

Complex **4** has been previously prepared by Girolami and co-workers by treatment of [TiCp*Cl_3] with 3 equiv of $LiBH_4$ in diethyl ether at –78 ºC.[32] In this procedure, complex **4** was isolated in 48% yield after successive crystallizations in toluene to remove a more soluble impurity. Remarkably, a green compound [Ti(η^5-C_5H_5)(BH_4)$_2$] similar to **7** was obtained in the reaction of [Ti(η^5-C_5H_5)Cl_3] with excess $LiBH_4$, but detailed characterization data for this complex have not been published in the literature.[18a]

The reactions of the trihalide compounds [TiCp*X_3] with $LiBH_4$ in tetrahydrofuran are mild when compared with those of $LiAlH_4$, and significant gas evolution was not visually observed in the preparation of the titanium(III) complexes **4**–**7**. This is consistent with $LiBH_4$ being a milder reducing agent than $LiAlH_4$.[33,34] Indeed, a solution of the titanium(III) complex **4** in tetrahydrofuran readily reacted with $LiAlH_4$ to cleanly give the titanium(II) derivative **1**. Most likely, the reaction occurs by replacement of the tetrahydridoborato units by tetrahydridoaluminato ligands and subsequent reduction of the resultant titanium(III) species by H_2 formation. Noteworthy, the reaction of [TiCp*Cl_3] with lithium tetrahydridogallate in tetrahydrofuran at room temperature occurred immediately with vigorous gas elimination. The formation of metallic gallium was visually observed in the reaction mixture, in accord with the decrease in thermal stability of the $LiGaH_4$ reagent,[35] and a pure compound could not be isolated from the resultant black solution.

Complexes **4**–**7** were characterized by spectral and analytical methods, as well as by X-ray crystallographic determinations for **6** and **7**. The crystal structure and spectroscopic data of **4** have been previously reported.[32] The ^{1}H NMR spectra of complexes **4** and **5** display one slightly broad resonance signal for the η^5-C_5Me_5 ligands at δ = 2.60 ($\Delta\nu_{1/2}$ = 35 Hz) and 2.59 ppm ($\Delta\nu_{1/2}$ = 20 Hz), respectively. The magnetic moment measurements for compounds **4** and **5** in [D_6]benzene at ambient temperature by the Evans Method gave

μ_{eff} = 1.38 and 1.28 μ_B per dimer [{TiCp*(BH_4)(μ-X)}$_2$].[36] These effective magnetic moments in solution at 295 K are significantly lower than that expected for the theoretical spin-only value (2.45 μ_B) for two non-interacting spins S = 1/2 in a dinuclear titanium(III) complex. This suggests an important antiferromagnetic coupling between the two metal centers which is consistent with the Ti–Ti distance of 3.452(1) Å determined in the crystal structure of **4**.[32] In contrast, the ^{1}H NMR spectrum of the mononuclear adduct [TiCp*(BH_4)$_2$(thf)] (**6**) in [D_6]benzene is silent and the Evans Method determination of its magnetic susceptibility confirms its paramagnetic nature (μ_{eff} of 1.87 μ_B) with one unpaired electron. Similarly, the ^{1}H NMR spectrum of the dinuclear titanium(III) complex **7** is silent and the magnetic moment measurement in [D_6]benzene at room temperature by the Evans Method gave a μ_{eff} of 2.36 μ_B, close to that expected (2.45 μ_B) for a dimer with two magnetically isolated Ti(III) ions. This is consistent with the long Ti–Ti distances of 3.787(1) and 3.832(1) Å obtained for the two independent molecules found in the X-ray crystal determination of compound **7**.

X-ray diffraction on a single crystal of **6** revealed a mononuclear structure with a titanium center coordinated by one η^5-C_5Me_5 ligand, four μ-H bridging hydrides of two BH_4 groups, and the oxygen atom of a tetrahydrofuran ligand (Figure 5). If the centroid of the η^5-C_5Me_5 ring is considered, the coordination geometry about the titanium atom can be described as distorted octahedral. The κ^2-coordinated BH_4 groups agree with the long Ti···B distances of 2.389(4) and 2.402(3) Å when compared with that found (2.220(9) Å) for the κ^3-BH_4 ligands of complex **4**.[32] The Ti–O bond length of 2.111(2) Å compares well with those found in other titanium(III) tetrahydrofuran adducts such as [Ti(η^5-C_5Me_5)Cl_2(thf)] (Ti–O = 2.083(2) Å).[11,37]

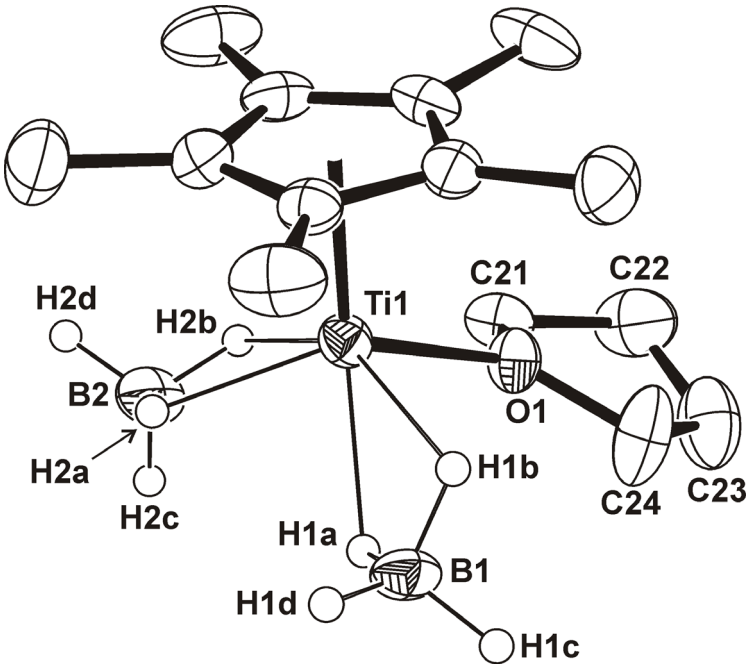

Figure 5. Perspective view of complex **6** with thermal ellipsoids at the 50% probability level. Hydrogen atoms of the η^5-C_5Me_5 and tetrahydrofuran ligands are omitted for clarity. Selected lengths (Å): Ti–O 2.111(2), Ti···B(1) 2.402(3), Ti···B(2) 2.389(4).

Crystals of **7** contain one and a half molecules in the asymmetric unit. Each molecule of **7** shows two [Ti(η^5-C_5Me_5)(BH_4)] units held together by two tetrahydridoborato ligands. However, while one molecule exhibits two different bridging BH_4 ligands, namely μ-κ^2:κ^1-BH_4 and μ-κ^1:κ^1-BH_4, between Ti(1) and Ti(2) centers (Figure 6), the second centrosymmetric molecule shows two μ-κ^1:κ^1-BH_4 between the Ti(3) atoms (Figure S3). The terminal BH_4 group linked to the six-coordinated titanium(2) atom shows a Ti(2)···B(2) distance of 2.364(5) Å similar to those found in complex **6**. However, the five-coordinated Ti(1) and Ti(3) centers exhibit shorter distances Ti(1)···B(1) and Ti(3)···B(3) (2.183(5) and 2.276(6) Å, respectively) for the κ^2-BH_4 terminal ligands.

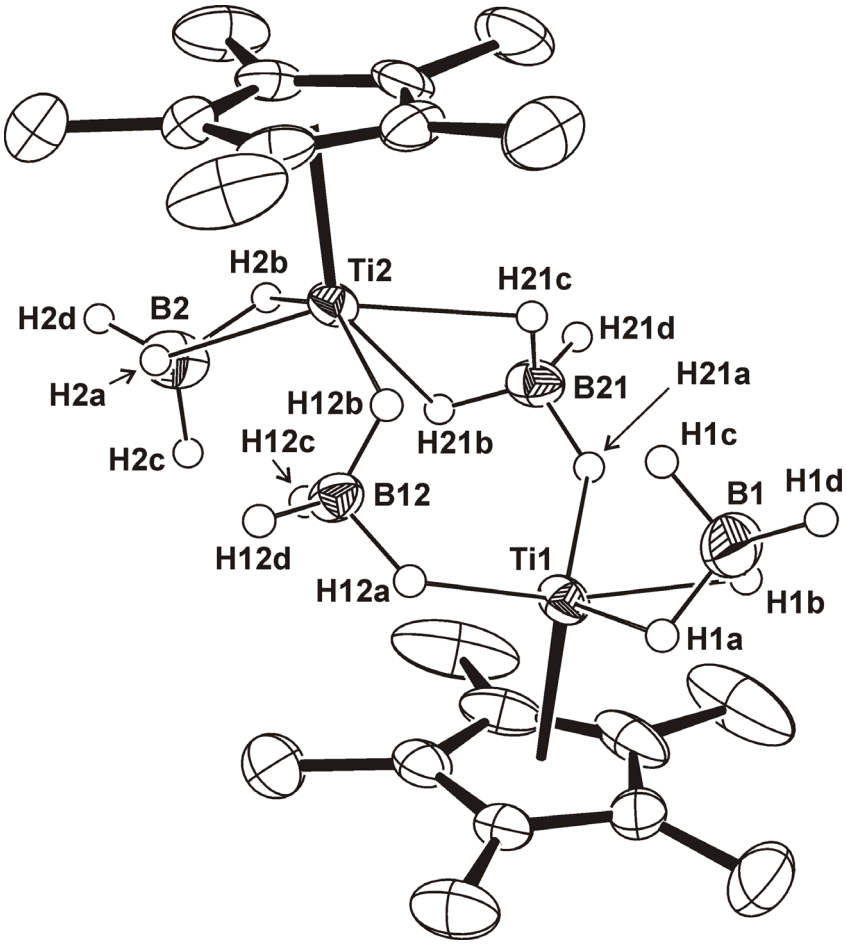

Figure 6. Perspective view for one of the two crystallographycally independent molecules of complex **7** with thermal ellipsoids at the 50% probability level. Hydrogen atoms of the η^5-C_5Me_5 ligands are omitted for clarity. Selected lengths (Å) for both independent molecules: Ti(1)···Ti(2) 3.787(1), Ti(1)···B(1) 2.183(5), Ti(2)···B(2) 2.364(5), Ti(1)···B(12) 2.641(4), Ti(1)···B(21) 2.716(5), Ti(2)···B(12) 2.446(4), Ti(2)···B(21) 2.448(5), Ti(3)···Ti(3)^{i} 3.832(1), Ti(3)···B(3) 2.276(6), Ti(3)···B(33) 2.561(4), Ti(3)···B(33)^{i} 2.589(4). Symmetry code: (i) 1 – *x*, 1 – *y*, –*z*.

The dimeric complex **7** readily dissolves in tetrahydrofuran to give a blue solution of the mononuclear adduct [TiCp*$(BH_4)_2$(thf)] (**6**) (Scheme 3). The analogous pyridine complex [TiCp*$(BH_4)_2$(py)] (**8**) was isolated as a green solid in 83% yield after addition of excess

pyridine (5 equiv) to a toluene solution of **7**. Similarly to **6**, the ^{1}H NMR spectrum of **8** in [D_6]benzene is silent and its paramagnetic nature was confirmed by an Evans Method determination of its magnetic susceptibility (μ_{eff} = 1.59 μ_B, 22 ºC, C_6D_6 solution). The reaction of **7** with triphenylphosphane (2 equiv) in [D_6]benzene was monitored by ^{1}H NMR spectroscopy. The spectra showed no reaction at temperatures lower than 65 ºC, when resonances for the adduct $BH_3(PPh_3)$ were detected. After 7 days at 80 ºC, the spectrum revealed resonance signals for $BH_3(PPh_3)$, H_2, and several broad resonance signals attributable to paramagnetic species. In a preparative scale reaction, the treatment of complex **7** with triphenylphosphane in hexane at 80 ºC led to the precipitation of adduct $BH_3(PPh_3)$ and a dark solution. Fractional crystallization of the solution components afforded a few red crystals of the dimeric diborane(6) complex [{TiCp*(μ-B_2H_6)}$_2$] (**9**) suitable for an X-ray crystal structure determination (vide infra).

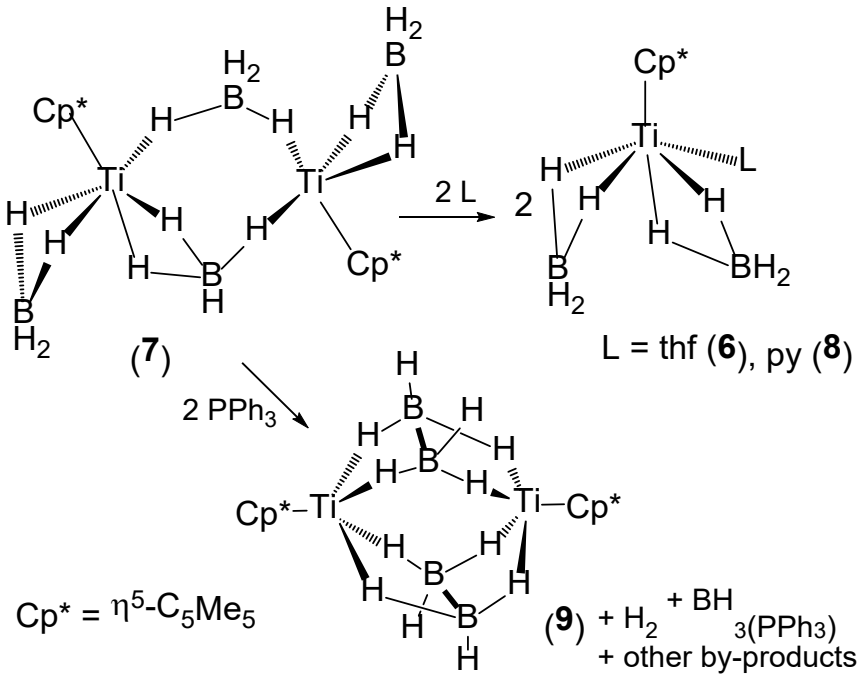

Scheme 3. Reactions of [{TiCp*(BH_4)(μ-BH_4)}$_2$] (**7**) with donor ligands L.

Compound **9** was independently prepared by treatment of the trimethyltitanium(IV) derivative [TiCp*Me_3] with an excess of a borane-tetrahydrofuran complex solution (Scheme 4). The reaction of [TiCp*Me_3] with 4 equiv of BH_3(thf) in toluene at room temperature led to gas evolution and formation of a dark-red solution from which dark-red crystals of the dinuclear complex [{TiCp*(BH_3Me)}$_2$(μ-B_2H_6)] (**10**) were obtained after crystallization (29% yield). In a separate experiment, the addition of a second solution of BH_3(thf) (1 equiv) in toluene to the former crude mixture containing **10** resulted in a red solution from which dark-red crystals of the diborane(6) complex **9** were isolated by crystallization (19% yield). The high solubility of compounds **9** and **10** in hydrocarbon solvents accounts for the low yields of crystalline samples which were used for characterization.

While several methyltrihydridoborato group 4 complexes have been prepared through the reaction of halide complexes with $LiBH_3Me$,[38,39,40] the formation of complex **10** presumably involves insertion of the BH_3 groups into the Ti–Me bonds. Thus, a hypothetical titanium(IV) intermediate [TiCp*(BH_3Me)$_3$] could be formed with a structure similar to that determined for the zirconium complex [ZrCp*(BH_3Me)$_3$].[40] While that zirconium(IV) complex is stable, the bis(cyclopentadienyl) compound [Zr(η^5-C_5H_5)$_2$(BH_3Me)$_2$] is only stable at low temperature and decomposes to give the hydride derivative [Zr(η^5-C_5H_5)$_2$H(BH_3Me)] and volatile diborane (BH_2Me)$_2$. Indeed, reduction to the titanium(III) derivative [Ti(η^5-C_5H_5)$_2$(BH_3Me)] was observed in the treatment of [Ti(η^5-C_5H_5)$_2$$Cl_2$] with excess $LiBH_3Me$.[39] In this reaction, the titanium(IV) is reduced to titanium(III) with presumably formation of H_2 and (BH_2Me)$_2$.

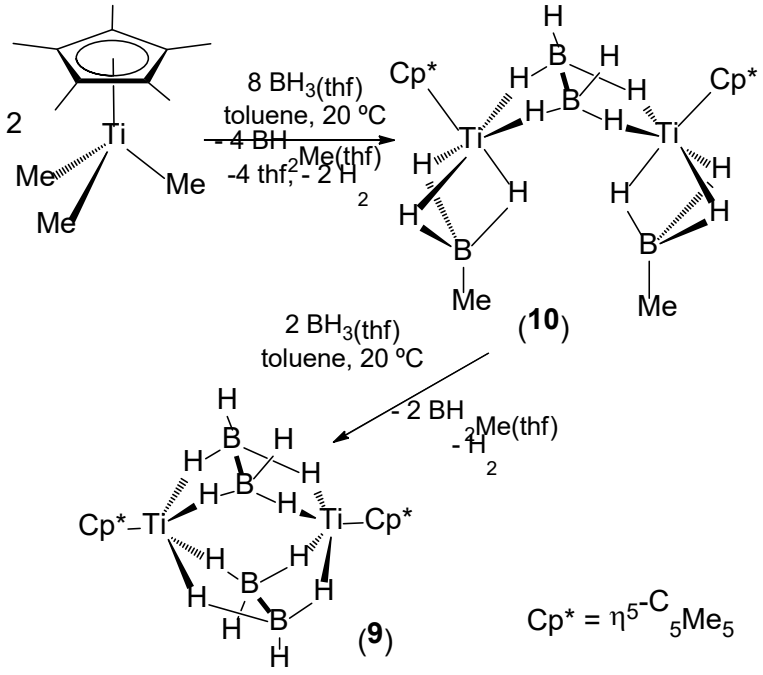

Scheme 4. Reactions of [TiCp*Me_3] with BH_3(thf).

The ^{1}H NMR spectrum of **10** in [D_6]benzene at room temperature shows two sharp singlet resonances for the methyl groups of the η^5-C_5Me_5 and BH_3Me ligands. In addition, the spectrum reveals two broad resonances at δ = –0.95 and –4.47 ppm for the hydrides of the κ^3-BH_3Me and μ-B_2H_6 ligands. The ^{11}B NMR spectra also show two broad signals at δ = 9.62 and 4.25 ppm. In contrast, the ^{1}H NMR spectrum of **9** in [D_6]benzene is silent and the paramagnetic nature of **9** with two unpaired electrons in the dinuclear structure was confirmed by an Evans method determination of the effective magnetic moment (μ_{eff} = 2.33 μ_B). The IR spectra of complexes **9** and **10** show strong bands at 2422 and 2426 cm^{-1} respectively, which are characteristic for the B–H stretching vibration of the $(B_2H_6)^{2-}$ ligand.[41]

Compound **9** crystallized in the *P*−1 space group with the half of two independent molecules in the asymmetric unit. Molecules of **9** lie on inversion centers in the midpoint of the Ti–Ti segments (Figures 7 and S4). There are not significant differences between

the two molecules (e.g., Ti(1)−Ti(1)^{i} and Ti(2)−Ti(2)^{ii} separations of 2.936(1) and 2.948(1) Å, respectively). Each titanium center exhibits a classical four-legged piano stool geometry with the legs occupied by four hydrides of two μ-B_2H_6 ligands. All the Ti···B distances are in the range 2.379(4)−2.400(3) Å, while the boron−boron bond lengths B(1)−B(2) and B(3)−B(4) are 1.800(5) and 1.803(5) Å, respectively. Overall, the structure of **9** is similar to those reported for diborane(6) complexes such as [{MCp*(μ-B_2H_6)}$_2$] (M = V,[42] Nb,[41] Ta[41]) which have been comprehensively reviewed by Ghosh and co-workers.[43]

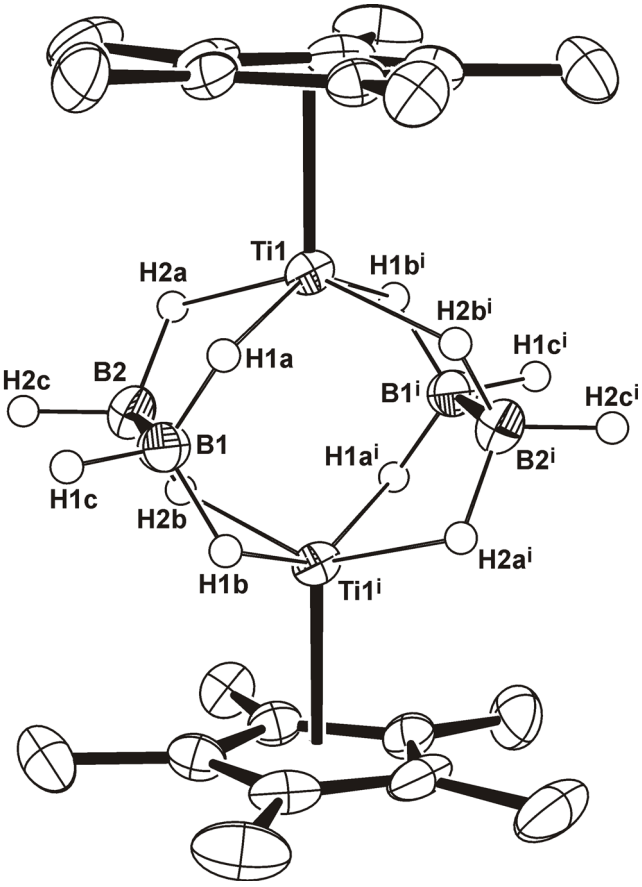

Figure 7. Perspective view for one of the two crystallographically independent molecules of **9** with thermal ellipsoids at the 50% probability level. The hydrogen atoms of the η^5-C_5Me_5 ligands are omitted for clarity. Selected lengths (Å) for both independent molecules: B(1)−B(2) 1.800(5), Ti(1)···Ti(1)^{i} 2.936(1), Ti(1)···B(1) 2.388(3),

Ti(1)···B(2) 2.386(4), Ti(1)···B(1)^{i} 2.396(3), Ti(1)···B(2)^{i} 2.400(3), B(3)−B(4) 1.803(5), Ti(2)···Ti(2)^{ii} 2.948(1), Ti(2)···B(3) 2.379(4), Ti(2)···B(4) 2.398(4), Ti(2)···B(3)^{ii} 2.396(3), Ti(2)···B(4)^{ii} 2.396(3). Symmetry code: (i) 1 – *x*, 1 – *y*, –*z*; (ii) 2 – *x*, –*y*, 1 – *z*.

The X-ray diffraction on single crystals of complex **10** revealed a dinuclear structure with two [Ti(η^5-C_5Me_5)(BH_3Me)] units linked by one μ-B_2H_6 ligand (Figure 8). The Ti···Ti separation of 4.147(1) Å in compound **10** is significantly longer than those found in the molecules of complex **9**. The κ^3-coordinated BH_3Me groups exhibit short Ti···B distances of 2.170(3) and 2.162(3) Å when compared with that (2.402(12) Å) found in [Ti(η^5-C_5H_5)$_2$(BH_3Me)] with a κ^2-coordinated BH_3Me.[39] The μ-B_2H_6 ligand of **10** shows a B−B bond length of 1.768(4) Å and bridges the titanium centers with Ti···B distances in the range 2.424(3)−2.451(3) Å, which are slightly longer than those of **9**. Most likely, the existence of two bridging B_2H_6 ligands between the two close titanium atoms in **9** produces these differences with respect to the open structure of complex **10**.

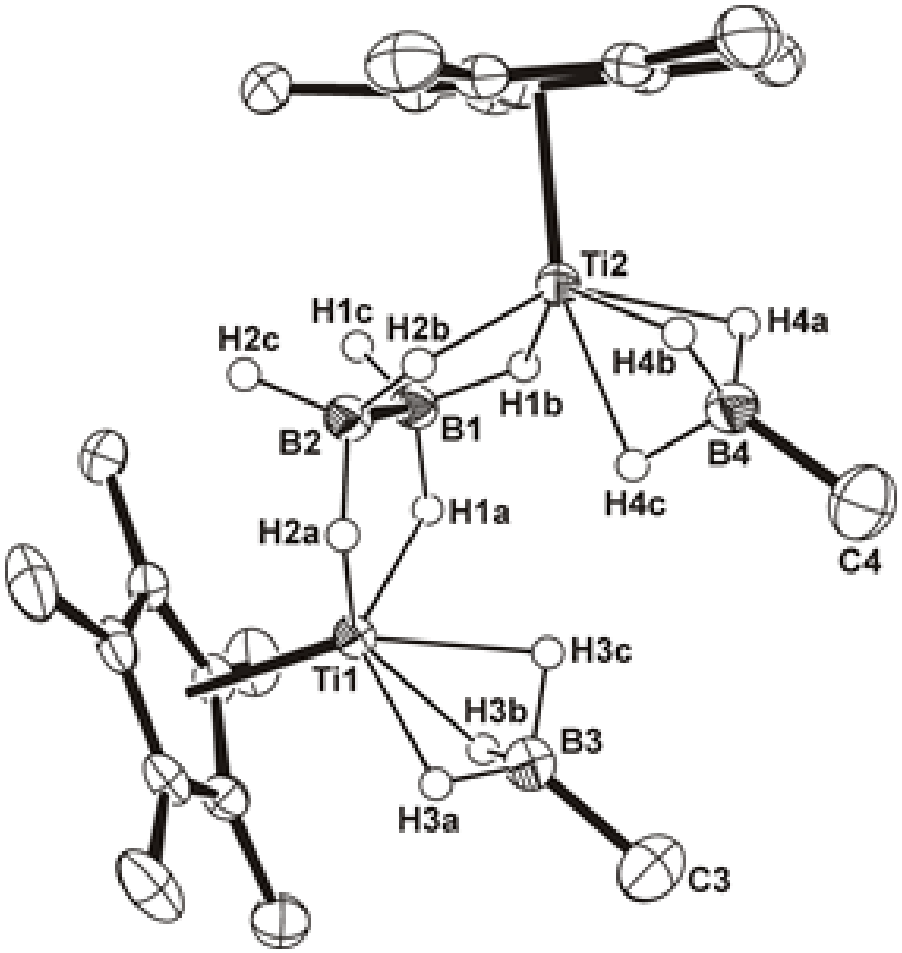

Figure 8 Perspective view of **10** with thermal ellipsoids at the 50% probability level. The hydrogen atoms of the methyl groups are omitted for clarity. Selected lengths (Å): Ti(1)···Ti(2) 4.147(1), Ti(1)···B(1) 2.451(3), Ti(1)···B(2) 2.430(3), Ti(1)···B(3) 2.170(3), Ti(2)···B(1) 2.428(3), Ti(2)···B(2) 2.424(3), Ti(2)···B(4) 2.162(3), B(1)–B(2) 1.768(4), B(3)–C(3) 1.575(4), B(4)–C(4) 1.569(4).

DFT calculations have been carried out to understand the electronic structure of complexes **9** and **10** and to explain their magnetic data. Initially, the singlet and triplet versions of complex **10** were calculated assuming, from the ligand charges, that the titanium atoms are Ti(III). The reorganization of the X-ray geometries is pretty low upon DFT optimization (Table S11 of the Supporting Information), thus it seems that the

starting charge/oxidation state guess *i.e.* Ti(III) was a good option. The calculations for **10** show that the singlet species is slightly lower (*ca.* 2 kcal mol^{-1}) in energy than the triplet analog. This compound is certainly an open-shell singlet, in which one unpaired electron can be localized on each Ti atom: one pointing up (α) and the other pointing down (β). Figure 9 (a, b) shows the SOMOs corresponding to this electronic distribution. This electron arrangement indicates this species should be diamagnetic, as observed experimentally. Additionally, Figure 9c represents the spin density on the molecule, which appears located on both metal centers, although some spin polarization is observed on the central B_2H_6 ligand. Considering the donor/acceptor NBO orbitals, two clear interactions can be identified where the B–H units, present both in the BH_3Me and in the B_2H_6 ligands, donate electron density to the empty *d* orbitals of the titanium centers (Figure S6).

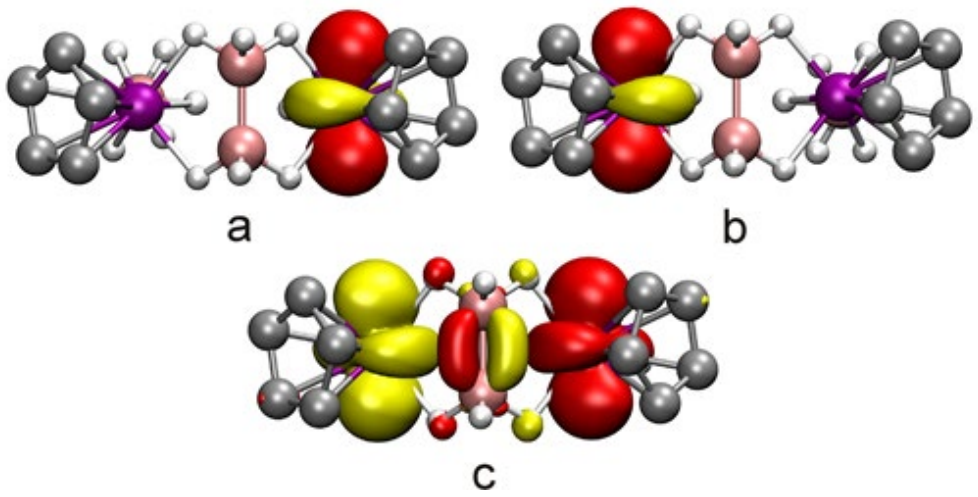

Figure 9. 3D representation of the SOMOs (a, b) and the spin density (c) for compound **10**. Methyl groups of the η^5-C_5Me_5 ligands are omitted for clarity.

Compound **9** was also analyzed by DFT calculations in the same way as **10**, describing the structure both as a singlet or a triplet species. A quite low reorganization was found

upon geometry optimization (Table S9), indicating that the titanium(III) guess was a good starting point. In this case the triplet structure is lower in energy by almost 3 kcal mol^{-1}. This electron distribution implies that each Ti atom has one unpaired electron pointing in the same orientation (α), so this compound should be expected to be paramagnetic, as observed in the experimental magnetic measurements. Figure 10 shows the SOMOs (a, b) and the spin density (c) for compound **9**.The paramagnetic nature of complex **9** was rather unexpected since the analogous group 5 compounds [{MCp*(μ-B_2H_6)}$_2$] (M = V, Nb, Ta) exhibit a diamagnetic character. Indeed, theoretical calculations on the ground state of [{VCp*(μ-B_2H_6)}$_2$] revealed an open-shell singlet, in which one unpaired electron can be localized on each vanadium atom, in addition to a V-V bond.[42] The donor/acceptor NBO interactions in complex **9** are simpler than those described above for **10** in accord to the existence of two identical diborane(6) bridging ligands. As shown in Figure S7, the full dianionic B_2H_6 units of **9**, through their B–H NBO orbitals, donate electron density to the empty *d* orbitals of the titanium centers.

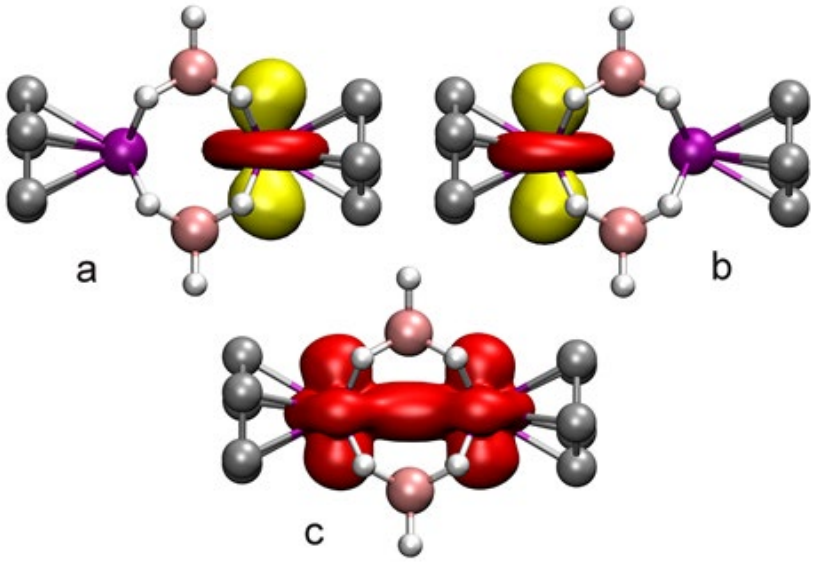

Figure 10. 3D representation of the SOMOs (a, b) and the spin density (c) for compound **9**. Methyl groups of the η^5-C_5Me_5 ligands are omitted for clarity.

Conclusions

Several low-valent half-sandwich titanium species have been prepared by reduction of trihalide complexes [TiCp*X_3] (X = Cl, Br) with $LiEH_4$ (E = Al, B) in ethereal solvents. The treatment with the strong reductant $LiAlH_4$ leads to the hydride-bridged heterometallic complexes [{TiCp*(μ-H)}$_2${(μ-H)$_2$AlX(L)}$_2$] (L = thf, X = Cl, Br; L = OEt_2, X = Cl). Theoretical studies on those bimetallic compounds reveal an open-shell singlet ground state in which an additional Ti–Ti bond has been established and can be described as true titanium(II) species. The strong electron density donation from the Ti–Ti bond to the empty *s* orbitals of the Al atoms stabilizes those compounds, which represent unprecedented examples for early transition metals containing σ-accepting (Z-type) ligands. While many complexes with this type of ligands are known for the electron-rich late transition metals, the electron density donation of metal–metal bonds to Lewis acid ligands, as those shown in our compounds, could be common for bi- or multimetallic low-valent early transition metal derivatives. In contrast, the reactions of the trihalides [TiCp*X_3] with the milder reductant $LiBH_4$ smoothly produce paramagnetic titanium(III) complexes stabilized with tetrahydridoborato ligands. Similarly, the treatment of the trimethyltitanium(IV) complex [TiCp*Me_3] with excess BH_3(thf) leads to the titanium(III) derivative [{TiCp*(μ-B_2H_6)}$_2$] via an intermediate [{TiCp*(BH_3Me)}$_2$(μ-B_2H_6)]. While the former bis(diborane(6)) compound has a triplet structure in spite of the short Ti–Ti separation, the latter diborane(6) intermediate with a very long Ti–Ti distance is an open-shell singlet.

Experimental Section

General Comments. All manipulations were carried out under argon atmosphere using Schlenk line or glovebox techniques. Toluene and hexane were distilled from Na/K alloy just before use. Tetrahydrofuran and diethyl ether were distilled from purple solutions of sodium benzophenone just prior to use. [D_6]benzene was dried with Na/K alloy and distilled before use. Oven-dried glassware was repeatedly evacuated with a pumping system (ca. 1×10^{-3} Torr) and subsequently filled with inert gas. Lithium tetrahydridoaluminate ($LiAlH_4$, 95%), and borane-tetrahydrofuran complex solution (BH_3(thf), 1.0 M in thf) were purchased from Aldrich and used as received. Lithium tetrahydridoborate ($LiBH_4$, ≥95%, Aldrich) was ground with a mortar and pestle until a very fine powder was obtained. Pyridine (Aldrich) was distilled from CaH_2. Triphenylphosphane was purchased from Aldrich and sublimed under vacuum prior to use. [$TiCp^*X_3$] (X = Cl,[24] Br,[24] Me[44]) and $LiGaH_4$[45] were prepared according to published procedures.

Samples for infrared spectroscopy were prepared as KBr pellets, and the spectra were obtained using an FT-IR Perkin-Elmer SPECTRUM 2000 spectrophotometer. ^{1}H and $^{13}C\{^1H\}$ NMR spectra were recorded on a Varian Unity-300, Mercury-300, or Unity-500 Plus spectrometers. ^{11}B NMR spectra were obtained using a Bruker AV300 spectrometer. Chemical shifts (δ) in the ^{1}H and $^{13}C\{^1H\}$ NMR spectra are given relative to residual protons or to carbon of the solvent, C_6D_6 (^{1}H: δ = 7.15; ^{13}C: δ = 128.0). Chemical shifts (δ) in the ^{11}B NMR spectra are given relative to $BF_3(OEt_2)$ as external reference. The effective magnetic moments in solution were determined by the Evans NMR method at 295 K (using a 300 MHz instrument with a field strength of 7.05 Tesla).[36] Melting points were determined in sealed capillary tubes under argon and are uncorrected. Microanalyses

(C, H, N) were performed in a Perkin Elmer CHNS/O 2400 or Leco CHNS-932 microanalyzers.

Synthesis of [{TiCp*(μ-H)}$_2${(μ-H)$_2$AlCl(thf)}$_2$] (1). A 150 mL Schlenk tube was charged with [TiCp*Cl$_3$] (0.60 g, 2.08 mmol), LiAlH$_4$ (0.16 g, 4.14 mmol), and tetrahydrofuran (20 mL) at room temperature. Vigorous gas evolution ensued. The reaction mixture was stirred for 20 h to give a dark-blue suspension. The volatile components were removed under reduced pressure and the resultant solid was extracted with toluene (25 mL). After filtration, the volatile components of the filtrate were removed under reduced pressure to afford **1** as a dark-blue solid (0.57 g, 85%). IR (KBr, cm^{-1}): $\tilde{\nu}$ 2971 (m), 2905 (vs), 2854 (s), 1488 (w), 1429 (m), 1376 (vs), 1261 (w), 1105 (m), 1024 (s), 874 (w), 792 (s), 772 (s), 622 (w), 443 (w). ^{1}H NMR (500 MHz, C$_6$D$_6$, 20 ºC, δ): 4.53 (m, 4H; OC*H*$_2$CH$_2$), 3.71 (m, 4H; OC*H*$_2$CH$_2$), 2.31 (s, 30H; C$_5$Me$_5$), 1.56 (m, 4H; OCH$_2$C*H*$_2$), 1.05 (m, 4H; OCH$_2$C*H*$_2$), the μ-H resonance signals were not observed. ^{13}C{^{1}H} NMR (125 MHz, C$_6$D$_6$, 20 ºC, δ): 114.5 (*C*$_5$Me$_5$), 71.5 (O*C*H$_2$CH$_2$), 71.2 (O*C*H$_2$CH$_2$), 25.3 (OCH$_2$*C*H$_2$), 24.7 (OCH$_2$*C*H$_2$), 14.2 (C$_5$*Me*$_5$). Anal. Calcd for C$_{28}$H$_{52}$Al$_2$Cl$_2$O$_2$Ti$_2$ (M_w = 641.31): C 52.44, H 8.17. Found: C 52.01, H 8.34.

Synthesis of [{TiCp*(μ-H)}$_2${(μ-H)$_2$AlBr(thf)}$_2$] (2). In a fashion similar to the preparation of **1**, [TiCp*Br$_3$] (0.30 g, 0.71 mmol) and LiAlH$_4$ (0.057 g, 1.42 mmol) were reacted in tetrahydrofuran (20 mL) for 20 h to give **2** as a dark-blue solid (0.16 g, 62%). IR (KBr, cm^{-1}): $\tilde{\nu}$ 2964 (m), 2904 (s), 2856 (m), 1485 (w), 1433 (m), 1376 (m), 1261 (w), 1067 (w), 1026 (m), 1009 (m), 915 (w), 865 (vs), 802 (m), 729 (w), 694 (w), 445 (w). ^{1}H NMR (500 MHz, C$_6$D$_6$, 20 ºC, δ): 4.55 (m, 4H; OC*H*$_2$CH$_2$), 3.72 (m, 4H; OC*H*$_2$CH$_2$), 2.30 (s, 30H; C$_5$Me$_5$), 1.58 (m, 4H; OCH$_2$C*H*$_2$), 1.06 (m, 4H; OCH$_2$C*H*$_2$), the μ-H resonance signals were not observed. ^{13}C{^{1}H} NMR (125 MHz, C$_6$D$_6$, 20 ºC, δ): 114.9

(C_5Me_5), 71.7 (OCH_2CH_2), 71.4 (OCH_2CH_2), 25.5 (OCH_2CH_2), 25.0 (OCH_2CH_2), 14.4 (C_5Me_5). Anal. Calcd for $C_{28}H_{52}Al_2Br_2O_2Ti_2$ (M_w = 730.23): C 46.06, H 7.18. Found: C 46.05, H 7.32.

Synthesis of [{TiCp*(μ-H)}$_2${(μ-H)$_2$AlCl(OEt$_2$)}$_2$] (3). A solution of [TiCp*Cl_3] (0.30 g, 1.04 mmol) in diethyl ether (25 mL) was slowly added to a suspension of $LiAlH_4$ (0.080 g, 2.08 mmol) in diethyl ether (100 mL) at 0 ºC. The reaction mixture was allowed to warm to room temperature and was stirred for 20 h to give a dark-brown suspension. The volatile components were removed under reduced pressure and the resultant solid was extracted with toluene (25 mL). After filtration, the volatile components of the toluene solution were removed under reduced pressure to give a dark-brown oily solid. This solid was dissolved in hexane (25 mL) and the solvent was removed under vacuum to afford **3** as a brown powder (0.19 g, 55%). Alternatively, the hexane solution was concentrated under reduced pressure to ca. 10 mL and was cooled to –35 ºC to give a very small fraction (0.015 g, 4%) of dark-blue crystals of **3**·0.5C_6H_{14}, which were used for NMR spectroscopy characterization and an X-ray crystal structure determination. ^{1}H NMR (500 MHz, C_6D_6, 20 ºC, δ): 4.41 (m, 4H; OCH_2CH_3), 3.59 (m, 4H; OCH_2CH_3), 2.27 (s, 30H; C_5Me_5), 1.32 (m, 6H; OCH_2CH_3), 0.83 (m, 6H; OCH_2CH_3), the μ-H resonance signals were not observed. ^{13}C{^{1}H} NMR (125 MHz, C_6D_6, 20 ºC, δ): 114.6 (C_5Me_5), 69.3 (OCH_2CH_3), 65.3 (OCH_2CH_3), 14.1 (OCH_2CH_3), 14.0 (C_5Me_5 and OCH_2CH_3).

Synthesis of [{TiCp*(BH$_4$)(μ-Cl)}$_2$] (4).[32] A 150 mL Schlenk tube was charged with [TiCp*Cl_3] (0.50 g, 1.73 mmol), $LiBH_4$ (0.079 g, 3.45 mmol), and tetrahydrofuran (25 mL). The reaction mixture was stirred at room temperature for 20 h to give a blue solution. The volatile components were removed under reduced pressure and the resultant solid was extracted with toluene (35 mL). After filtration, the volatile components of the filtrate

were removed under reduced pressure to give **4** as a green solid (0.25 g, 62%). IR (KBr, cm^{-1}): $\tilde{\nu}$ 2972 (s), 2913 (vs), 2857 (m), 2525 (vs), 2286 (m), 2135 (m), 2069 (m), 1487 (m), 1453 (m), 1425 (m), 1380 (s), 1298 (s), 1263 (m), 1201 (s), 1097 (w), 1023 (s), 801 (s), 729 (w), 536 (s), 455 (m). ^{1}H NMR (300 MHz, C_6D_6, 20 ºC, δ): 2.60 (s br., $\Delta\nu_{1/2}$ = 35 Hz; C_5Me_5). Anal. Calcd for $C_{20}H_{38}B_2Cl_2Ti_2$ (M_w = 466.26): C 51.46, H 8.20. Found: C 51.03, H 8.25. The effective magnetic moment of **4** was determined to be 1.38 μ_B (based on a unit formula of $C_{20}H_{38}B_2Cl_2Ti_2$) on a C_6D_6 solution.

Synthesis of [{TiCp*(BH$_4$)(μ-Br)}$_2$] (5). In a fashion similar to the preparation of **4**, [TiCp*Br_3] (0.30 g, 0.71 mmol) and $LiBH_4$ (0.033 g, 1.42 mmol) were reacted in tetrahydrofuran (25 mL) for 20 h to afford **5** as a green solid (0.14 g, 74%). IR (KBr, cm^{-1}): $\tilde{\nu}$ 2952 (s), 2911 (vs), 2857 (m), 2527 (vs), 2274 (w), 2132 (m), 2066 (w), 1487 (m), 1453 (w), 1426 (m), 1378 (s), 1298 (vs), 1199 (s), 1067 (w), 1022 (s), 801 (m), 728 (s), 540 (m), 461 (w). ^{1}H NMR (300 MHz, C_6D_6, 20 ºC, δ): 2.59 (s br., $\Delta\nu_{1/2}$ = 20 Hz; C_5Me_5). Anal. Calcd for $C_{20}H_{38}B_2Br_2Ti_2$ (M_w = 555.68): C 43.23, H 6.89. Found: C 42.92, H 6.30. The effective magnetic moment of **5** was determined to be 1.28 μ_B (based on a unit formula of $C_{20}H_{38}B_2Br_2Ti_2$) on a C_6D_6 solution.

Synthesis of [TiCp*(BH$_4$)$_2$(thf)] (6). A 150 mL ampule (Teflon stopcock) was charged with [TiCp*Cl_3] (1.00 g, 3.45 mmol), $LiBH_4$ (0.40 g, 17.2 mmol), and tetrahydrofuran (35 mL). The reaction mixture was stirred at 85 ºC for 20 h and the volatile components were removed under reduced pressure. The resultant solid was extracted with toluene (20 mL). After filtration, tetrahydrofuran (20 mL) and hexane (10 mL) were added to the filtrate and the resultant solution was cooled to –35 ºC for 7 days to afford **6** as dark-blue crystals (0.19 g, 26%). IR (KBr, cm^{-1}): $\tilde{\nu}$ 2973 (m), 2911 (m), 2854 (w), 2425 (vs), 2290 (m), 2220 (w), 2071 (m), 1990 (w), 1486 (w), 1424 (m), 1383 (s), 1345 (s), 1261 (w),

1024 (s), 813 (s), 521 (w), 507 (w), 425 (s), 414 (s). Anal. Calcd for $C_{14}H_{31}B_2OTi$ (M_w = 284.89): C 59.02, H 10.97. Found: C 59.29, H 10.47. The effective magnetic moment of **6** was determined to be 1.87 μ_B (based on a unit formula of $C_{14}H_{31}B_2OTi$) on a C_6D_6 solution.

Synthesis of [{TiCp*(BH$_4$)(μ-BH$_4$)}$_2$] (7). *Caution! Compound 7 is pyrophoric and can be spontaneously combust on contact with air, so special care should be taken when handling this substance and its residues. Method A:* A 150 mL ampule (Teflon stopcock) was charged with [TiCp*Cl_3] (1.00 g, 3.45 mmol), $LiBH_4$ (0.40 g, 17.2 mmol), and tetrahydrofuran (35 mL). The reaction mixture was stirred at 85 ºC for 20 h to give a blue solution. The volatile components were removed under reduced pressure and the resultant solid was extracted with toluene (25 mL). After filtration, the volatile components were removed under reduced pressure to afford a dark-blue solid. Sublimation at 75 ºC under vacuum (0.1 Torr) gave huge dark-blue crystals of **7** (0.30 g, 41%). *Method B:* A 150 mL Schlenk tube was charged with [TiCp*Cl_3] (1.00 g, 3.45 mmol), finely powdered $LiBH_4$ (0.40 g, 17.2 mmol), and toluene (35 mL). The reaction mixture was stirred at room temperature for 20 h to give a dark solution and a gray solid. After filtration, the volatile components of the solution were removed under reduced pressure to give **7** (0.59 g, 80%) as a dark-blue powder (mp 67-68 ºC). IR (KBr, cm^{-1}): $\tilde{\nu}$ 2979 (s), 2958 (s), 2913 (vs), 2727 (w), 2536 (s), 2445 (vs), 2397 (m), 2238 (m), 2137 (w), 2097 (m), 2026 (w), 1922 (w), 1485 (m), 1456 (m), 1426 (m), 1379 (s), 1303 (m), 1262 (m), 1223 (m), 1123 (vs), 1068 (w), 1024 (vs), 984 (m), 802 (m), 707 (m), 511 (m), 424 (w). Anal. Calcd for $C_{20}H_{46}B_4Ti_2$ (M_w = 425.56): C 56.45, H 10.89. Found: C 56.38, H 10.83. The effective magnetic moment of **7** was determined to be 2.36 μ_B (based on a unit formula of $C_{20}H_{46}B_4Ti_2$) on a C_6D_6 solution.

Synthesis of [TiCp*(BH$_4$)$_2$(py)] (8). Pyridine (0.14 g, 1.76 mmol) was slowly added to a solution of **7** (0.15 g, 0.35 mmol) in toluene (25 mL). The reaction mixture was stirred at room temperature for 3 days. The volatile components of the resultant solution were removed under reduced pressure to give **8** as a green powder (0.17 g, 83%). IR (KBr, cm^{-1}): $\tilde{\nu}$ 2955 (m), 2914 (m), 2858 (w), 2433 (s), 2394 (vs), 2338 (s), 2227 (m), 2151 (m), 2110 (m), 1602 (s), 1485 (s), 1459 (w), 1443 (vs), 1380 (m), 1215 (m), 1119 (vs), 1063 (m), 1009 (m), 763 (vs), 704 (vs), 636 (m), 449 (m), 426 (m). Anal. Calcd for $C_{15}H_{28}B_2NTi$ (M_w = 291.88): C 61.72, H 9.67, N 4.80. Found: C 61.78, H 9.65; N 5.51. The effective magnetic moment of **8** was determined to be 1.59 μ_B (based on a unit formula of $C_{15}H_{28}B_2NTi$) on a C_6D_6 solution.

Synthesis of [{TiCp*(μ-B$_2$H$_6$)}$_2$] (9). A solution of BH_3(thf) (3.93 mL, 1.0 M in thf, 3.93 mmol) in toluene (10 mL) was added to a solution of [TiCp*Me$_3$] (0.30 g, 1.31 mmol) in toluene (30 mL). After stirring for 20 h at room temperature, a second solution of BH_3(thf) (1.31 mL, 1.0 M in thf, 1.31 mmol) in toluene (10 mL) was added. The reaction mixture was stirred again for 20 h at room temperature to give a dark-red solution. The volume of the solution was concentrated under reduced pressure to ca. 4 mL. After filtration, the resultant red solution was cooled to –35 ºC to give **9** as dark-red crystals which were isolated by filtration. The filtrate was cooled at –35 ºC for 5 days to afford a second crop of crystals. The combined yield of **9** was 19% (0.052 g). IR (KBr, cm^{-1}): $\tilde{\nu}$ 2954 (m), 2911 (s), 2856 (m), 2422 (vs), 2369 (w), 2071 (m), 1992 (w), 1956 (w), 1486 (w), 1426 (w), 1381 (s), 1333 (m), 1261 (w), 1024 (m), 811 (m), 502 (w), 423 (m). Anal. Calcd for $C_{20}H_{42}B_4Ti_2$ (M_w = 421.53): C 56.99, H 10.04. Found: C 56.88, H 9.25. The effective magnetic moment of **9** was determined to be 2.33 μ_B (based on a unit formula of $C_{20}H_{42}B_4Ti_2$) on a C_6D_6 solution.

Synthesis of [{TiCp*(BH$_3$Me)}$_2$(μ-B$_2$H$_6$)] (10). A solution of BH$_3$(thf) (3.93 mL, 1.0 M in thf, 3.93 mmol) in toluene (10 mL) was added to a solution of [TiCp*Me$_3$] (0.30 g, 1.31 mmol) in toluene (30 mL). The reaction mixture was stirred for 20 h at room temperature to give a dark-red solution. The volume of the solution was concentrated under reduced pressure to ca. 4 mL. After filtration, the resultant red solution was cooled to –35 ºC for 2 days to afford **10** as dark-red crystals (0.085 g, 29%). IR (KBr, cm^{-1}): $\tilde{\nu}$ 2943 (s), 2904 (vs), 2426 (s), 2195 (w), 2136 (w), 1990 (vs), 1857 (m), 1835 (m), 1488 (w), 1455 (w), 1429 (w), 1378 (vs), 1348 (vs), 1261 (w), 1026 (m), 950 (w), 801 (m), 459 (s), 422 (w). ^{1}H NMR (500 MHz, C$_6$D$_6$, 20 ºC, δ): 1.91 (s, 30H; C$_5$Me$_5$), 0.76 (s, 6H; BMe), –0.95 (s br., $\Delta\nu_{1/2}$ = 221 Hz, 6H; BH$_3$), –4.47 (s br., $\Delta\nu_{1/2}$ = 305 Hz; 6H; BH$_3$). ^{13}C{^{1}H} NMR (125 MHz, C$_6$D$_6$, 20 ºC, δ): 122.6 (*C*$_5$Me$_5$), 13.5 (C$_5$*Me*$_5$), the B*C*H$_3$ resonance signal was not observed. ^{11}B NMR (128 MHz, C$_6$D$_6$, 20 ºC, δ): 9.78 (s br.; BH$_3$), 4.00 (s br.; BH$_3$). Anal. Calcd for C$_{22}$H$_{48}$B$_4$Ti$_2$ (M_w = 451.60): C 58.51, H 10.71. Found: C 59.17, H 10.14.

X-ray crystal structure determinations. Dark-blue crystals of compounds **1**, **3**·0.5C$_6$H$_{14}$, and **7** were grown from *n*-hexane solutions at −35 °C. Dark-blue crystals of **2** and dark-red crystals of **9** and **10** were grown from toluene solutions at –35 ºC. Dark-blue crystals of **6** were grown from a toluene/tetrahydrofuran/*n*-hexane (2/2/1) solution at –35 ºC. The crystals were removed from the Schlenk tubes and covered with a layer of a viscous perfluoropolyether (FomblinY). A suitable crystal was selected with the aid of a microscope, mounted on a cryoloop, and immediately placed in the low temperature nitrogen stream of the diffractometer. The intensity data sets were collected at 150 K on a Bruker-Nonius KappaCCD diffractometer equipped with an Oxford Cryostream 700 unit. Crystallographic data for all the complexes are presented in Tables S1 and S2 of the Supporting Information.

The structures were solved, using the WINGX package,[46] by direct methods (**6** and **10**), Patterson (**7**) (SHELXS-2013),[47] or intrinsic phasing methods (**1**, **2**, **3** and **9**) (SHELXT),[48] and refined by least-squares against F^2 (SHELXL-2014/7).[47] Compound **3** crystallized with a half molecule of *n*-hexane, whereas **1** and **2** crystallized as solvent-free molecules. In the crystallographic studies of **1**–**3**, all non-hydrogen atoms were anisotropically refined. All hydrogen atoms were included, positioned geometrically, and refined employing a riding model, except those of the hydride ligands (H(1), H(2), H(3), H(4), H(5) and H(6)) which were located in the difference Fourier map and refined isotropically.

Crystals of **7** contained one and a half molecules in the asymmetric unit (Z = 6, in the $P2_1/c$ space group), whereas compound **9** crystallized in the $P\bar{1}$ space group with the half of two independent molecules in the asymmetric unit (Z = 2). All non-hydrogen atoms in **6**, **7**, **9** and **10** were anisotropically refined. All hydrogen atoms in these crystals were placed geometrically and refined by using a riding model, except those linked to boron atoms which were located in the Fourier map and isotropically refined. Additionally in the study of **7**, SADI restraints were applied to the separations between the hydrogen atoms (H(33a), H(33b), H(33c) and H(33d)) bound to B(33), and carbon atoms of the pentamethylcyclopentadienyl ring (C(31)-C(40)) linked to Ti(3) were also restrained with DELU instructions.

Computational Details. All the structures have been fully optimized in gas phase employing the Gaussian09 suite of programs[49] and using the unrestricted formalism of the B3LYP functional.[50] All the Al, B, C, H and Ti atoms are described with the triple-ζ all electron basis set of Ahlrichs and co-workers.[51] The computed energies have been corrected with the D3 empirical dispersion method of Grimme.[52] The NBO analysis has

been carried out at the same level of theory as above with the NBO 3.1 program included in Gaussian09.[53]

Acknowledgements

We thank the Spanish MCIU (PGC2018-094007-B-I00 and PGC2018-093863-B-C21) and Universidad de Alcalá (CCG20/CC-007) for financial support of this research. E.d.H. thanks the Universidad de Alcalá for a doctoral fellowship. J.J. acknowledges the Spanish Structures of Excellence María de Maeztu program through grant MDM-2017–0767.

Conflict of interest

The authors declare no conflict of interest.

References

[1] M. Manβen, L. L. Schafer, *Chem. Soc. Rev.* **2020**, *49*, 6947–6994.

[2] E. P. Beaumier, A. J. Pearce, X. Y. See, I. A. Tonks, *Nat. Rev. Chem.* **2019**, *3*, 15–34.

[3] a) H. Tsurugi, K. Mashima, *Acc. Chem. Res.* **2019**, *52*, 769–779; b) H. Tsurugi, K. Mashima, *Chem. Eur. J.* **2019**, *25*, 913–919.

[4] a) T. V. RajanBabu, W. A. Nugent, *J. Am. Chem. Soc.* **1994**, *116*, 986–997; b) A. Gansäuer, H. Bluhm, *Chem. Rev.* **2000**, *100*, 2771–2788; c) A. F. Barrero, J. F. Quílez del Moral, E. M. Sánchez, J. F. Arteaga, *Eur. J. Org. Chem.* **2006**, 1627–1641; d) A. Gansäuer, J. Justicia, C.-A. Fan, D. Worgull, F. Piestert in *Topics in Current Chemistry*, Vol. 279 (Ed.: M. J. Krische*),* Springer, Berlin, Germany **2007**, pp. 25–52; e) S. P. Morcillo, D. Miguel, A. G. Campaña, L. Álvarez de Cienfuegos, J. Justicia, J. M. Cuerva, *Org. Chem. Front*. **2014**, *1*, 15–33; f) A. Rosales, I. Rodríguez-García, J. Muñoz-Bascón,

E. Roldan-Molina, N. M. Padial, L. Pozo-Morales, M. García-Ocaña, J. E. Oltra, *Eur. J. Org. Chem.* **2015**, 4567–4591; g) M. Castro-Rodríguez, I. Rodríguez-García, R. N. Rodríguez-Maecker, L. Pozo-Morales, J. E. Oltra, A. Rosales-Martínez, *Org. Process Res. Dev.* **2017**, *21*, 911–923; h) J. M. Botubol-Ares, M. J. Durán-Peña, J. R. Hanson, R. Hernández-Galán, I. G. Collado, *Synthesis* **2018**, *50*, 2163–2180; i) T. McCallum, X. Wu, S. Lin, *J. Org. Chem.* **2019**, *84*, 14369–14380; j) W. A. Nugent, T. V. RajanBabu, *Angew. Chem. Int. Ed.* **2021**, *60*, 2194–2201; *Angew. Chem.* **2021**, *133*, 2222–2229; k) A. Rosales-Martínez, L. Pozo-Morales, E. Díaz-Ojeda, M. Castro-Rodríguez, I. Rodríguez-García, *J. Org. Chem.* **2021**, *86*, 1311–1329.

[5] Z. W. Davis-Gilbert, I. A. Tonks, *Dalton Trans.* **2017**, *46*, 11522–11528.

[6] S. Okamoto, *Chem. Rec.* **2016**, *16*, 857–872.

[7] T. Saito, H. Nishiyama, H. Tanahashi, K. Kawakita, H. Tsurugi, K. Mashima, *J. Am. Chem. Soc.* **2014**, *136*, 5161–5170.

[8] a) R. Jungst, D. Sekutowski, J. Davis, M. Luly, G. Stucky, *Inorg. Chem.* **1977**, *16*, 1645–1655; b) K. Mach, V. Varga, G. Schmid, J. Hiller, U. Thewalt, *Collect. Czech. Chem. Commun.* **1996**, *61*, 1285–1294; c) M. Klahn, P. Arndt, A. Spannenberg, A. Gansäuer, U. Rosenthal, *Organometallics* **2008**, *27*, 5846–5851; d) M. Krizan, J. Honzicek, J. Vinklarek, Z. Ruzickova, M. Erben, *New J. Chem*. **2015**, *39*, 576–588.

[9] a) P. C. Wailes, R. S. P. Coutts, H. Weigold, *Organometallic Chemistry of Titanium, Zirconium and Hafnium*, Academic Press, New York, **1974**; b) R. Poli, *Chem. Rev.* **1991**, *91*, 509–551.

[10] a) W. Hao, X. Wu, J. Z. Sun, J. C. Siu, S. N. MacMillan, S. Lin, *J. Am. Chem. Soc.* **2017**, *139*, 12141–12144; b) W. Hao, J. H. Harenberg, X. Wu, S. N. MacMillan, S. Lin, *J. Am. Chem. Soc.* **2018**, *140*, 3514–3517; c) S. Okamoto, T. Yamada, Y. Tanabe, M. Sakai,

Organometallics **2018**, *37*, 4431–4438; d) X. Wu, W. Hao, K.-Y. Ye, B. Jiang, G. Pombar, Z. Song, S. Lin, *J. Am. Chem. Soc.* **2018**, *140*, 14836–14843.

[11] M. García-Castro, C. García-Iriepa, E. del Horno, A. Martín, M. Mena, A. Pérez-Redondo, M. Temprado, C. Yélamos, *Inorg. Chem*. **2019**, *58*, 5314–5324.

[12] E. del Horno, R. Jiménez-Aparicio, M. Mena, A. Pérez-Redondo, J. L. Priego, C. Yélamos, *Inorg. Chem*. **2020**, *59*, 3740–3752.

[13] For selected examples, see: a) E. J. Corey, R. L. Danheiser, S. Chandrasekaran, *J. Org. Chem.* **1976**, *41*, 260–265; b) K. Isagawa, K. Tatsumi, Y. Otsuji, *Chem. Lett.* **1976**, 1145–1148; c) K. Isagawa, K. Tatsumi, H. Kosugi, Y. Otsuji, *Chem. Lett.* **1977**, 1017–1020; d) C. H. Wong, C. W. Hung, H. N. C. Wong, *J. Organomet. Chem.* **1988**, *342*, 9–14; e) L. K. Woo, J. A. Hays, V. G. Young, C. L. Day, C. Caron, F. D´Souza, K. M. Kadish, *Inorg. Chem.* **1993**, *32*, 4186–4192; f) H. S. Lee, H. Y. Lee, *Bull. Korean Chem. Soc.* **2000**, *21*, 451–452.

[14] M. J. Butler, M. R. Crimmin, *Chem. Commun.* **2017**, *53*, 1348–1365.

[15] a) G. L. Soloveichik, B. M. Bulychev, *Russ. Chem. Rev.* **1983**, *52*, 43–60; b) E. B. Lobkovskii, G. L. Soloveichik, A. I. Sisov, B. M. Bulychev, A. I. Gusev, N. I. Kirillova, *J. Organomet. Chem.* **1984**, *265*, 167–173; c) E. B. Lobkovskii, G. L. Soloveichik, B. M. Bulychev, R. G. Gerr, Y. T. Struchkov, *J. Organomet. Chem.* **1984**, *270*, 45–51; d) V. K. Bel'sky, A. I. Sizov, B. M. Bulychev, G. L. Soloveichik, *J. Organomet. Chem.* **1985**, *280*, 67–80; e) A. I. Sizov, I. V. Molodnitskaya, B. M. Bulychev, E. V. Evdokimova, G. L. Soloveichik, A. I. Gusev. E. B. Chuklanova, V. I. Andrianov, *J. Organomet. Chem.* **1987**, *335*, 323–330; f) A. I. Sisov, I. V. Molodnitskaya, B. M. Bulychev, E. V. Evdokimova, V. K. Bel´skii, G. L. Soloveichik, *J. Organomet. Chem.* **1988**, *344*, 293–301; g) B. M.

Bulychev, *Polyhedron* **1990**, *9*, 387–408; h) A. I. Sizov, T. M. Zvukova, B. M. Bulychev, V. K. Belsky, *J. Organomet. Chem.* **2000**, *603*, 167–173.

[16] a) L. J. Guggenberger, F. N. Tebbe, *J. Am. Chem. Soc.* **1973**, *95*, 7870–7872; b) V. V. Burlakov, K. Kaleta, T. Beweries, P. Arndt, W. Baumann, A. Spannenberg, V. B. Shur, U. Rosenthal, *Organometallics* **2011**, *30*, 1157–1161; c) J. Thomas, M. Klahn, A. Spannenberg, T. Beweries, *Dalton Trans.* **2013**, *42*, 14668–14672; d) R. Sun, J. Liu, S. Yang, M. Chen, N. Sun, H. Chen, X. Xie, X. You, S. Li, Y. Liu, *Chem. Commun.* **2015**, *51*, 6426–6429; e) A. C. Brown, A. B. Altman, T. D. Lohrey, S. Hohloch, J. Arnold, *Chem. Sci.* **2017**, *8*, 5153–5160; f) K. J. Blakeney, P. D. Martin, C. H. Winter, *Organometallics* **2020**, *39*, 1006–1013; g) K. Sugita, M. Yamashita, *Organometallics* **2020**, *39*, 2125–2129.

[17] B. M. Bulychev, S. E. Tokareva, G. L. Soloveichick, E. V. Evdokimova, *J. Organomet. Chem.* **1979**, *179*, 263–273.

[18] For reviews on tetrahydridoborato complexes, see: a) T. J. Marks, J. R. Kolb, *Chem. Rev.* **1977**, *77*, 263–293; b) V. D. Makhaev, *Russ. Chem. Rev.* **2000**, *69*, 727–746; c) M. Besora, A. Lledós, *Struct. Bond.* **2008**, *130*, 149–202.

[19] a) T. P. Fehlner, J.-F. Halet, J.-Y. Saillard, *Molecular Clusters: A Bridge to Solid-State Chemistry*, Cambridge University Press, Cambridge, **2007**; b) T. P. Fehlner, *Organometallics* **2000**, *19*, 2643–2651; c) S. Kar, A. N. Pradhan, S. Ghosh, *Coord. Chem. Rev.* **2021**, *436*, 213796; and references therein.

[20] B. Bogdanović, M. Schwickardi, *J. Alloys Comp.* **1997**, *253–254*, 1–9.

[21] For recent reviews, see: a) T. J. Frankcombe, *Chem. Rev.* **2012**, *112*, 2164–2178; b) E. Callini, Z. Ö. K. Atakli, B. C. Hauback, S. Orimo, C. Jensen, M. Dornheim, D. Grant, Y. W. Cho, P. Chen, B. Hjörvarsson, P. de Jongh, C. Weidenthaler, M. Baricco, M.

Paskevicius, T. R. Jensen, M. E. Bowden, T. S. Autrey, A. Züttel, *Appl. Phys. A.* **2016**, *122*, 353; c) C. Milanese, S. Garroni, F. Gennari, A. Marini, T. Klassen, M. Dornheim, C. Pistidda, *Metals* **2018**, *8*, 567; d) N. A. Ali, M. Ismail, *Int. J. Hydrogen Energy* **2021**, *46*, 766–782; e) Z. Ren, X. Zhang, Z. Huang, J. Hu, Y. Li, S. Zheng, M. Gao, H. Pan, Y. Liu, *Chem. Eng. J.* **2022**, *427*, 131546.

[22] a) B. Bogdanović, U. Eberle, M. Felderhoff, F. Schüth, *Scr. Mater.* **2007**, *56*, 813–816; b) S. Zhang, C. Lu, N. Takeichi, T. Kiyobayashi, N. Kuriyama, *Int. J. Hydrogen Energy* **2011**, *36*, 634–638.

[23] E. del Horno, J. Jover, M. Mena, A. Pérez-Redondo, C. Yélamos, *Chem. Eur. J.* **2019**, *25*, 7096–7100.

[24] G. H. Llinás, M. Mena, F. Palacios, P. Royo, R. Serrano, *J. Organomet. Chem.* **1988**, *340*, 37–40.

[25] Deposition numbers 2019995 (for **1**), 2019996 (for **2**), 2019997 (for **3**), 2019998 (for **6**), 2019999 (for **7**), 202000 (for **9**) and 202001 (for **10**) contain(s) the supplementary crystallographic data for this paper. These data are provided free of charge by the joint Cambridge Crystallographic Data Centre and Fachinformationszentrum Karlsruhe.

[26] *Holleman-Wiberg: Inorganic Chemistry* (Ed. N. Wiberg), 1st ed. in English, Academic Press, New York, **2001**, pp. 1756–1759.

[27] L. Yang, D. R. Powell, R. P. Houser, *Dalton Trans.* **2007**, 955–964.

[28] B. Cordero, V. Gómez, A. E. Platero-Prats, M. Revés, J. Echeverría, E. Cremades, F. Barragán, S. Álvarez*, Dalton Trans.* **2008**, *40*, 2832–2838.

[29] For reviews, see: a) B. R. Barnett, J. S. Figueroa, *Chem. Commun.* **2016**, *52*, 13829–13839; b) G. Bouhadir, D. Bourissou, *Struct. Bond.* **2017**, *171*, 141–202; c) H. Kameo,

H. Nakazawa, *Chem. Rec.* **2017**, *17*, 268–286; d) D. You, F. P. Gabbai, *Trends in Chemistry* **2019**, *1*, 485–496.

[30] M. Greño, E. del Horno, M. Mena, A. Pérez-Redondo, V. Varela-Izquierdo, C. Yélamos, *Inorg. Chem.* **2017**, *56*, 11220–11229.

[31] G. Parkin, *Organometallics* **2006**, *25*, 4744–4747.

[32] D. Y. Kim, Y. You, G. S. Girolami, *J. Organomet. Chem.* **2008**, *693*, 981–986.

[33] N. G. Connelly, W. E. Geiger, *Chem. Rev*. **1996**, *96*, 877–910.

[34] Z. M. Heiden, A. P. Lathem, *Organometallics* **2015**, *34*, 1818–1827.

[35] N. N. Greenwood, A. Earnshaw, *Chemistry of the Elements*, 2nd ed. Butterworth Heinemann, Oxford, **1998**, pp. 232–233.

[36] a) D. F. Evans, *J. Chem. Soc.* **1959**, 2003–2005; b) S. K. Sur, *J. Magn. Reson.* **1989**, *82*, 169–173; c) G. A. Bain, J. F. Berry, *J. Chem. Educ.* **2008**, *85*, 532–536.

[37] T. Oswald, M. Schmidtmann, R. Beckhaus, *Z. Kristallogr. NCS* **2016**, *231*, 637–639.

[38] W. K. Kot, N. M. Edelstein, A. Zalkin, *Inorg. Chem.* **1987**, *26*, 1339–1341.

[39] F.-C. Liu, K.-Y. Chen, J.-H. Chen, G.-H. Lee, S.-M. Peng, *Inorg. Chem.* **2003**, *42*, 1758–1763.

[40] F.-C. Liu, C.-C. Yang, S.-C. Chen, G.-H. Lee, S.-M. Peng, *Dalton Trans.* **2008**, 3599–3604.

[41] S. K. Bose, K. Geetharani, V. Ramkumar, S. M. Mobin, S. Ghosh, *Chem. Eur. J.* **2009**, *15*, 13483–13490.

[42] A. Haridas, S. Kar, B. Raghavendra, T. Roisnel, V. Dorcet, S. Ghosh, *Organometallics* **2020**, *39*, 58–65.

[43] R. Borthakur, K. Saha, S. Kar, S. Ghosh, *Coord. Chem. Rev.* **2019**, *399*, 213021.

[44] M. Mena, P. Royo, R. Serrano, M. A. Pellinghelli, A. Tiripicchio, *Organometallics* **1989**, *8*, 476–482.

[45] A. E. Shirk, D. F. Shriver, *Inorg. Synth.* **1977**, *17*, 45–47.

[46] L. J. Farrugia, *J. Appl. Crystallogr.* **2012**, *45*, 849–854.

[47] G. M. Sheldrick, *Acta Crystallogr., Sect. C: Struct. Chem.* **2015**, *71*, 3–8.

[48] G. M. Sheldrick, *Acta Crystallogr., Sect. A: Found. Adv.* **2015**, *71*, 3–8.

[49] M. J. Frisch, G. W. Trucks, H. B. Schlegel, G. E. Scuseria, M. A. Robb, J. R. Cheeseman, G. Scalmani, V. Barone, B. Mennucci, G. A. Petersson, H. Nakatsuji, M. Caricato, X. Li, H. P. Hratchian, A. F. Izmaylov, J. Bloino, G. Zheng, J. L. Sonnenberg, M. Hada, M. Ehara, K. Toyota, R. Fukuda, J. Hasegawa, M. Ishida, T. Nakajima, Y. Honda, O. Kitao, H. Nakai, T. Vreven, J. J. A. Montgomery, J. E. Peralta, F. Ogliaro, M. Bearpark, J. J. Heyd, E. Brothers, K. N. Kudin, V. N. Staroverov, R. Kobayashi, J. Normand, K. Raghavachari, A. Rendell, J. C. Burant, S. S. Iyengar, J. Tomasi, M. Cossi, N. Rega, N. J. Millam, M. Klene, J. E. Knox, J. B. Cross, V. Bakken, C. Adamo, J. Jaramillo, R. Gomperts, R. E. Stratmann, O. Yazyev, A. J. Austin, R. Cammi, C. Pomelli, J. W. Ochterski, R. L. Martin, K. Morokuma, V. G. Zakrzewski, G. A. Voth, P. Salvador, J. J. Dannenberg, S. Dapprich, A. D. Daniels, Ö. Farkas, J. B. Foresman, J. V. Ortiz, J. Cioslowski, D. J. Fox, *Gaussian09, Revision D.01*, Gaussian, Inc.: Wallingford CT, **2009**.

[50] a) A. D. Becke, *J. Chem. Phys.* **1993**, 98, 5648–5652; b) C. Lee, W. Yang, R. G. Parr, *Phys. Rev. B* **1988**, 37, 785–789; c) B. Miehlich, A. Savin, H. Stoll, H. Preuss, *Chem. Phys. Lett.* **1989**, 157, 200–206.

[51] A. Schäfer, C. Huber, R. Ahlrichs, *J. Chem. Phys.* **1994**, 100, 5829–5835.

[52] S. Grimme, J. Antony, S. Ehrlich, H. Krieg, *J. Chem. Phys.* **2010**, 132, 154104–154119.

[53] E. D. Glendening, A. E. Reed, J. E. Carpenter, F. Weinhold, *NBO*, Version 3.1.

Entry for the Table of Contents

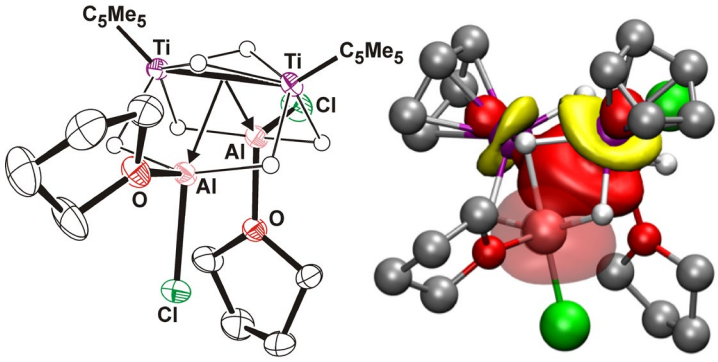

The structure and bonding of bimetallic half-sandwich titanium(III) and titanium(II) complexes stabilized by boron (BH_4^-, BH_3Me^-, $B_2H_6^{2-}$) or aluminum {(μ-H)$_2$AlXL)} hydride ligands are reported. DFT calculations on the hydride-bridged Ti(II)-Al compounds reveal unprecedented M→Z type interactions in early transition metal systems.